Journal of Renewable Energies

Revue des Energies Renouvelables

journal home page : https://revue.cder.dz/index.php/rer

Numerical study to predict optimal configuration of wavy fin and tube heat exchanger with various tube shapes

Farouk Tahrour [a,*], Fares Djeffal [b], Lyes Bordja [c], Abdelmoumene Hakim Benmachiche [d]

[a] *Department of physics, University of M'sila, 28000 M'sila, Algeria*

[b,c] *Department of Mechanical Engineering, University of Oum El Bouaghi, (04000) Oum El Bouaghi, Algeria*

[d] *Department of physics, university of Batna 1, Algeria*

**corresponding author, E-mail: farouk.tahrour@univ-msila.dz*

Tel.: +213 06 71 02 42 41

Abstract

This paper aims to investigate the influence of tube shapes on thermal-flow characteristics of sinusoidal wavy finned-tube heat exchangers. Two row staggered bundle with six geometries of tubes (four flat tube geometries, one oval tube and a circular tube) are analyzed for a range of $(1600 \leq Re \leq 4800)$. The inspection revealed that the heat flux and the pressure drop decrease with the tube flatness for all Reynolds values. However, the oval tube O1 reaches, for all Reynolds values, the lowest values of heat flux and pressure drop. Regarding the global performance criterion, the sinusoidal wavy fins with O1 shaped tubes reached the highest global performance values, being 14.8–24.4% and 31.6–36.3% higher than the fin with F1 and O2 tube geometry, respectively.

Keywords: Flat tube; Oval tube; Fluent; Heat exchanger; Optimization; Wavy fin.

1. Introduction

Currently, tubes with wavy fins bundle are widely used in industry, such as internal and external combustion engines, automobiles, geothermal energy and thermodynamic solar power plants. Because air-side thermal resistance makes up a larger portion of total thermal resistance (up to 90 percent) [1-2]. As a result, lowering the air-side resistance is critical. Among the techniques used to minimize this thermal resistance is the change in the bundle arrangement and shapes fins and tubes. To improve the overall heat transfer and flow characteristics of heat exchangers, a number of geometric parameters are applied [3-7]. On the other hand, changing the forms and configurations of the tubes in sinusoidal wavy fins, remains a viable strategy for improving heat transfer properties while incurring a pumping power penalty.

The liquid crystal thermography method was used by Fiebig et al. [8] to measure and compares the convective heat exchange and flow structure for three-row with plate FTHEs for circular and flat tube shapes. They found that longitudinal vortices result in a large heat exchange improvement (100%) for flat shaped tubes but only 10% for the case of circular tubes over a range of $\left(600 \le Re \le 3000\right)$. The commercial code FLUENT is used by Sun et al. [9] to evaluate the overall thermal performance of the elliptical and circular plate finned-tube bundle. The elliptical tube geometry with fins improves the heat transfer by 3.6-6.7%, according to the researchers. CFD modeling has also been used by Zeeshan et al. [1] to determine the thermo-hydraulic performance of tube bank with flat fins for small *Re* numbers (400-900). The authors considered the circular, oval and flat tube patterns for both types of tube arrangement. To improve the efficiency of heat exchangers, they advised reducing the flatness of flat shaped tubes and the axis ratio of oval tubes. The same tube patterns were investigated by Djeffal et al. [10] for the case of heat exchanger with annular finnes and a turbulent flow regime. The numerical findings demonstrate that when the axis ratio and tube flatness rise, the heat flux and Colburn factor increase while the friction factor decreases.

For the case of natural convection thermal exchange, Unger et al. [10] analyzed the impact of flat-tube shapes and dimensions on thermal-flow characteristics for four rows of annular FTHEs. It was found that, for staggered tube arrangement, the conventional circular tube and flat tube pattern (with an axis ratio of 1:2.1) gives the highest heat exchanger efficiency. He et al. [11] analyzed experimentally and numerically the gas side heat exchange and flow physics of circular and elliptic plate FTHEs and their results show that the heat transfer of the elliptical shaped-tubes was approximately 66% superior to that of the circular one.

Recently, Darbari and Alavi [12] applied the TEDM (Taguchi experiment design method) and statistical analysis of variance (ANOVA) to explore the impact of flat tube configurations (without fins). The findings demonstrate that, whereas the axial ratio has a significant impact on pressure drop, it has little impact on heat transfer characteristics. Numerical simulations were conducted by Alnakeeb et al., [13] using the CFD code FLUENT 17.2 to determine the convective heat transfer and fluid flow properties for a laminar flow regime having plate fins and six different aspect ratios (0.33 to 1) of flat tubes. When decreasing the tube flatness from 1 to 0.33 the pressure losses decrease by 33.7% and 57.3% and the global performance criterion by 52.9% and 111.5% for the range of $0.5 \le V_{in} \le 3.5\, m/s$.

For plain plate fins and flat tube shape (with aspect ratio of 0.4), Phu et al. [14] investigated numerically the impact of tube inclination angle and Re number in four row staggered bundle.

They observed that as the inclination angle of the flat tube is changed between 0 and 45°, the thermal flow performance increase because the minimum section of flow passage decreases, resulting in increased of air velocity.

Unfortunately, the majority of research studies have separately investigated the effect of tube ellipticity and flatness in FTHEs. Also, only Zeeshan et al. [1] and Djeffal et al. [10] numerically analyzed the heat transfer and flow physics in FTHEs using circular, oval, and flat shaped-tubes, whereas, in the case of sinusoidal wavy FTHEs, no research has been done on the influence of these tube forms. Hence, the purpose here is to examine the influence of tube shapes with sinusoidal wavy fins for two-row staggered bundles using the RNG $k-\varepsilon$ turbulence model of ANSYS FLUENT 18.2.

2. Model Descriptions

2.1. Physical Model

The dimensions and boundary conditions applied in the current computational domain are provided in (Fig. 1). To have a uniform velocity at the entrance, the inlet region is extended 10 times the fin spacing S_f, however, the outlet region is extended 30 times the fin spacing S_f. The solid bodies including the sinusoidal wavy fins were made of aluminum. The dimensions of the wavy fins are: fin thickness $t_f = 0.12$ mm, fin spacing $S_f = 1.7$ mm, wave amplitude $A = 1.75$ mm and wave number $N_w = 4$ waves. In this work, we examined six geometries of tubes with sinusoidal wavy fins for staggered arrangement (Fig. 2). The values of basic parameters of tube shapes with wavy FTHEs are summarized in Table 1.

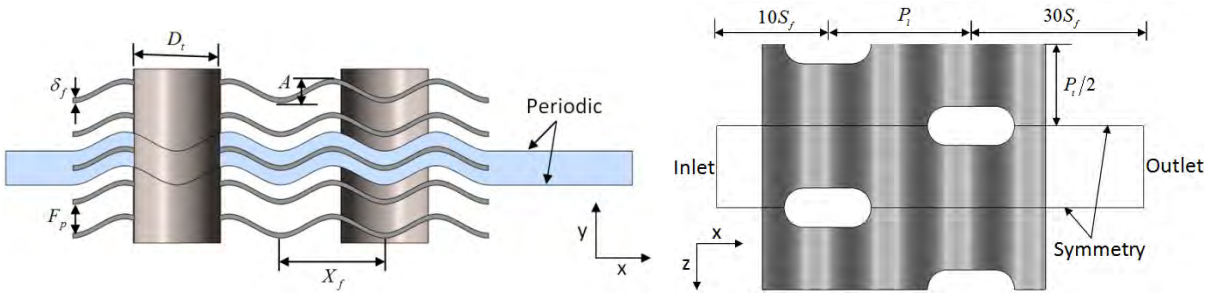

Fig 1. Geometrical parameters of the investigated sinusoidal wavy FTHEs.

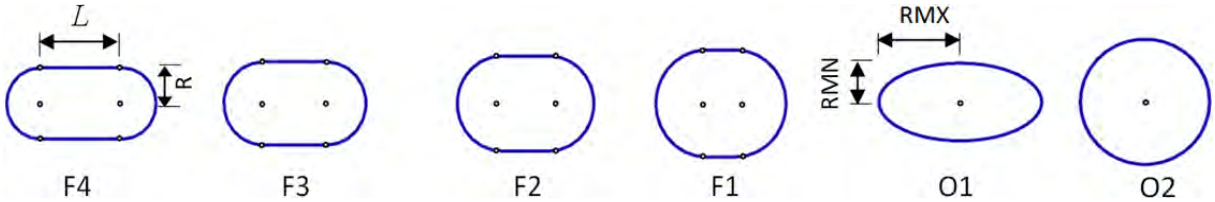

Fig 2. Geometries of all flat and oval tubes tested.

Table 1. Sinusoidal wavy fins and tube shape dimensions.

Tube Shape	Dimensions/mm			
	Radius R (mm)	Length L(mm)	Major axis radius RMX (mm)	Minor axis radius RMN (mm)
F1	3	7.335		
F2	3.5	5.764		
F3	4	4.193		
F4	4.5	2.622		
O1			7	3.345
O2 (circular)			5.33	5.33

2.2. Numerical solution

2.2.1. Governing Equations

Based on the hydraulic diameter of tubes, the Reynolds number is varied in the interval [1600-4800]. Therefore, the problem is assumed to be 3D, incompressible, and turbulent airflow. With these conditions, the conservation equations of mass, momentum and energy are written as follows:

$$\frac{\partial u_i}{\partial x_i} = 0 \tag{1}$$

$$\frac{\partial}{\partial x_j}\left(\rho u_i u_j + p\delta_{ij} - \mu\left(\frac{\partial u_i}{\partial x_j} + \frac{\partial u_j}{\partial x_i} - \frac{2}{3}\delta_{ij}\frac{\partial u_l}{\partial x_l} \right) + \rho_a \overline{u_i' u_j'} \right) = 0 \tag{2}$$

where:

$$-\rho_a \overline{u_i' u_j'} = \mu_t\left(\frac{\partial u_i}{\partial x_j} + \frac{\partial u_j}{\partial x_i} \right) - \frac{2}{3}\left(\rho_a k + \mu_t \frac{\partial u_i}{\partial x_i} \right)\delta_{ij} \tag{3}$$

Energy equation:

$$\frac{\partial(u_i(\rho_a E + p))}{\partial x_i} = \frac{\partial}{\partial x_i}((k_a + k_t)\frac{\partial T}{\partial x_i}) \tag{4}$$

where, E is the total energy and k_t is the turbulent thermal conductivity.

2.2.2. Boundary Conditions

Heat transfer and turbulent flow characteristics at the boundaries of the present computational domain, as illustrated in (Fig. 1), are shown in Table 2.

Table 2. Boundary conditions

Surface	T	V	P
Inlet	$T = C^{st}$ (293K)	$V = C^{st}$ (2–6m/s)	P_{atm}
Fin surfaces	Determined by Fluent	No slip	Determined by Fluent
Outer tube surface	$T = C^{st}$ (343K)	No slip	Determined by Fluent
Upper and lower faces of symmetry	$\frac{\partial T}{\partial y} = 0$	$\frac{\partial u}{\partial y} = \frac{\partial w}{\partial y} = 0,\ v = 0$	$\frac{\partial p}{\partial y} = 0$
Right and left sides of symmetry	$\frac{\partial T}{\partial z} = 0$	$\frac{\partial u}{\partial z} = \frac{\partial v}{\partial z} = 0,\ w = 0$	$\frac{\partial p}{\partial z} = 0$
Outlet	$\frac{\partial T}{\partial x} = 0$	$\frac{\partial u}{\partial x} = \frac{\partial v}{\partial x} = \frac{\partial w}{\partial x} = 0$	P_{atm}

2.2.3 Numerical Procedures

The ANSYS WORKBENCH 18.2 meshing tool is used to discretize the computational domain. To produce accurate results with little computational time, the mesh is kept as uniform and smooth (hexahedral) as possible as reported in Figure 3. Table 3 summarized the results of grid independence test.

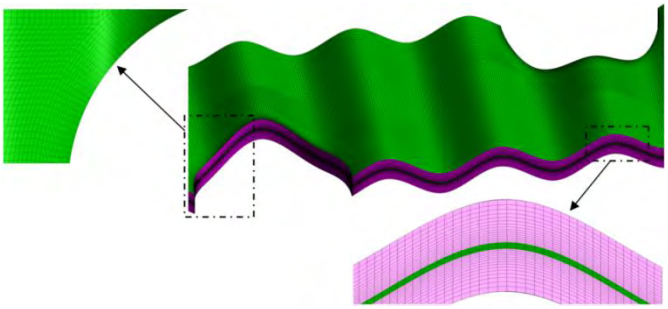

Fig 3. Mesh of the sinusoidal wavy fins with flat shaped tubes.

Table 3. Findings of the mesh independence study.

Mesh size	0.5×10^6	0.9×10^6	1.25×10^6	1.8×10^6
φ	1.1292	1.7089	1.7633	1.7789
ΔP	147.089	131.107	125.856	123.923

The air-side heat transfer rate of the sinusoidal wavy FTHXs is calculated as follows:

$$\varphi = \dot{m} c_p \left(T_{out} - T_{in} \right) \tag{5}$$

where $\dot{m} = \rho_a A_{in} u_{in}$ is the air mass flow rate.

Eventually, the global performance criterion G_{pc} gives the overall heat transfer rate of sinusoidal wavy FTHXs comparatively with the unit flow power consumption. This parameter is defined in Ref. [16] as follows:

$$G_{pc} = \frac{\varphi}{\Delta P \dot{V}} \tag{6}$$

3. Results

3.1 Validation of the Numerical Model

To conduct the validation, the calculated j and f factors in the range of $1600 \le Re \le 4800$ are compared against the experimental results of Youn and Kim [17] (Fig. 4). The validation was carried out with a two-row deep design, fin pitch 1.7 mm, wave amplitude 1.5 mm, and wavelength 10.82 mm. A good agreement is remarked in this figure with the results of Youn and Kim [17] with maximum deviations of 10.8% and 5.4% in j and f values, respectively.

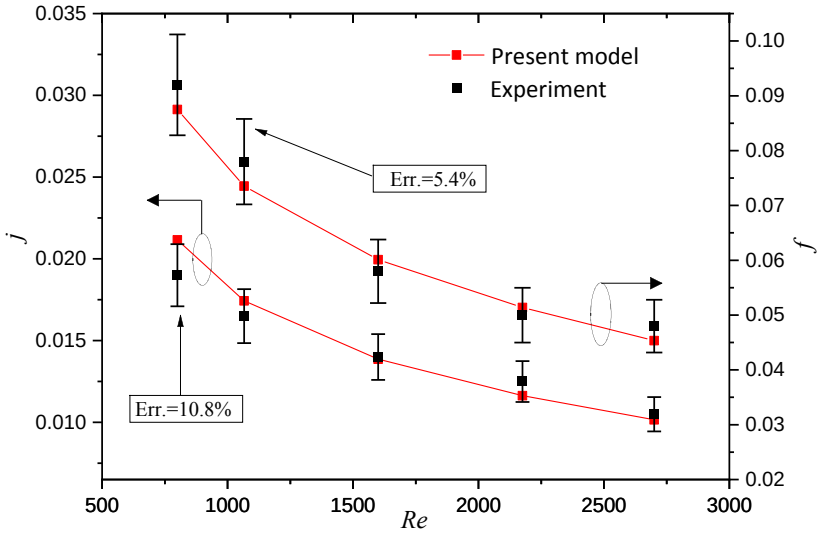

Fig 4. Validation against the experimental data of Youn and Kim [17].

3.2 Impact of Tube geometry on Flow Physics

To illuminate the effect of tube pattern on flow physics in staggered two-row with sinusoidal wavy FTHEs, it is important to plot the local distributions of the streamlines between and behind the tubes. For the six tube geometries, Fig. (5) illustrate the 2D distribution of the streamlines at Re= 4800. The effects of tube geometry manifest in fluid separation downstream of the wavy crest, its reattachment upstream of the following crest, and the consequent creation and encirclement of re-circulating cells in the valley regions. The size and strength of the recirculation zone become more pronounced as the flatness of the tube decreases. However, the largest recirculation zone is generated behind the circular tubes (O2).

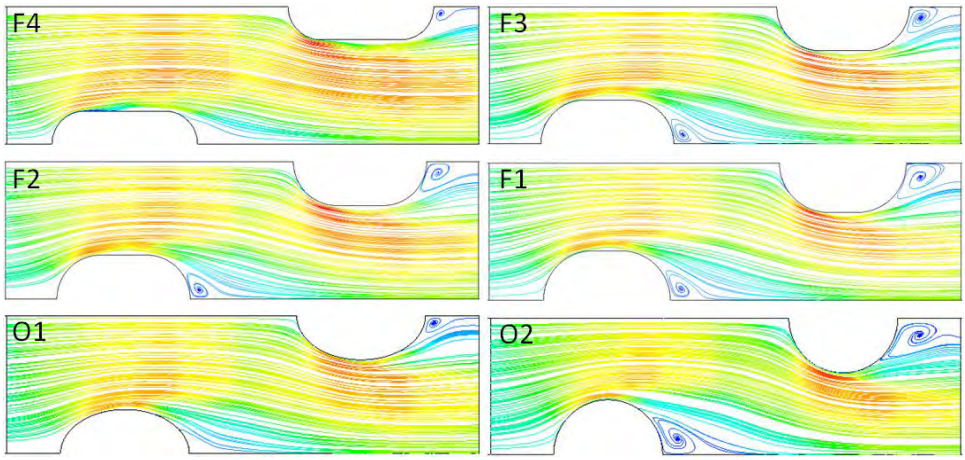

Fig 5. Streamlines behind the two rows for all tube shapes at Re= 4800.

3.3 Impact of tube geometry on thermal-flow characteristics

For fixed fin spacing of $S_f = 1.7\,\text{mm}$ and wavy fin dimensions, and for the range of $1600 \le Re \le 4800$, the impact of tube geometries on thermal-flow efficiency is presented and compared in this part of the paper. The variation of thermal flux φ vs. Re number of various tube shape are shown in Fig. 6(a). For all tube shapes, the heat transfer enhanced with *Re* due to the improvement of heat transfer with the air-flow velocity. Also, the heat transfer rate decrease with the tube flatness and wavy fins with oval tubes give the low values of thermal flux for all Re values. In fact, the F1 flat-tube geometry provides 4.7-6% and 3.9-6.3% higher heat flux than the F4 tube shape and the conventional circular tube (O2), respectively. This improvement in heat transfer is due to the increase in the maximum fluid velocity at the minimum flow-passage section between two adjacent tubes and the increase of the heat transfer area of sinusoidal wavy fins with the decrease of tube flatness. Fig. 6(b) shows the variation of the pressure losses ΔP for different tube geometries at various Reynolds number. As expected, for all Reynolds numbers, the ΔP values decreases as the tube flatness increase. Of all inspected tube shapes, O1 shaped tube with sinusoidal wavy fins provides 24.7–31.2% and 33.5–38.2% lower pressure drop as compared to the F1 and O2 shaped tube, respectively, because both recirculating vortices and drag force decreases with the tube axis ratio.

The goal of thermal device design is to provide a significant thermal transfer while minimizing pressure drop. Therefore, the global performance criterion G_{PC} is used here to evaluate and compare the overall efficiency between all tube shapes.

Fig. 6(c) depicts the variation of G_{pc} vs. the tube geometry for the *Re* range of [1600–4800]. Whatever the tube shape, G_{pc} is decreasing with the rise of *Re* due to the rapid increase in pressure drop with the slow rise of thermal transfer rate. As observed, G_{pc} increases with the

rise of tube flatness. However, for all *Re* values, the G_{pc} values given by wavy fins with the oval tubes O1 is the most substantial of all the other tube geometries, being 14.8–24.4% and 31.6–36.3% higher than the fin with F1 and O2 tube geometry, respectively.

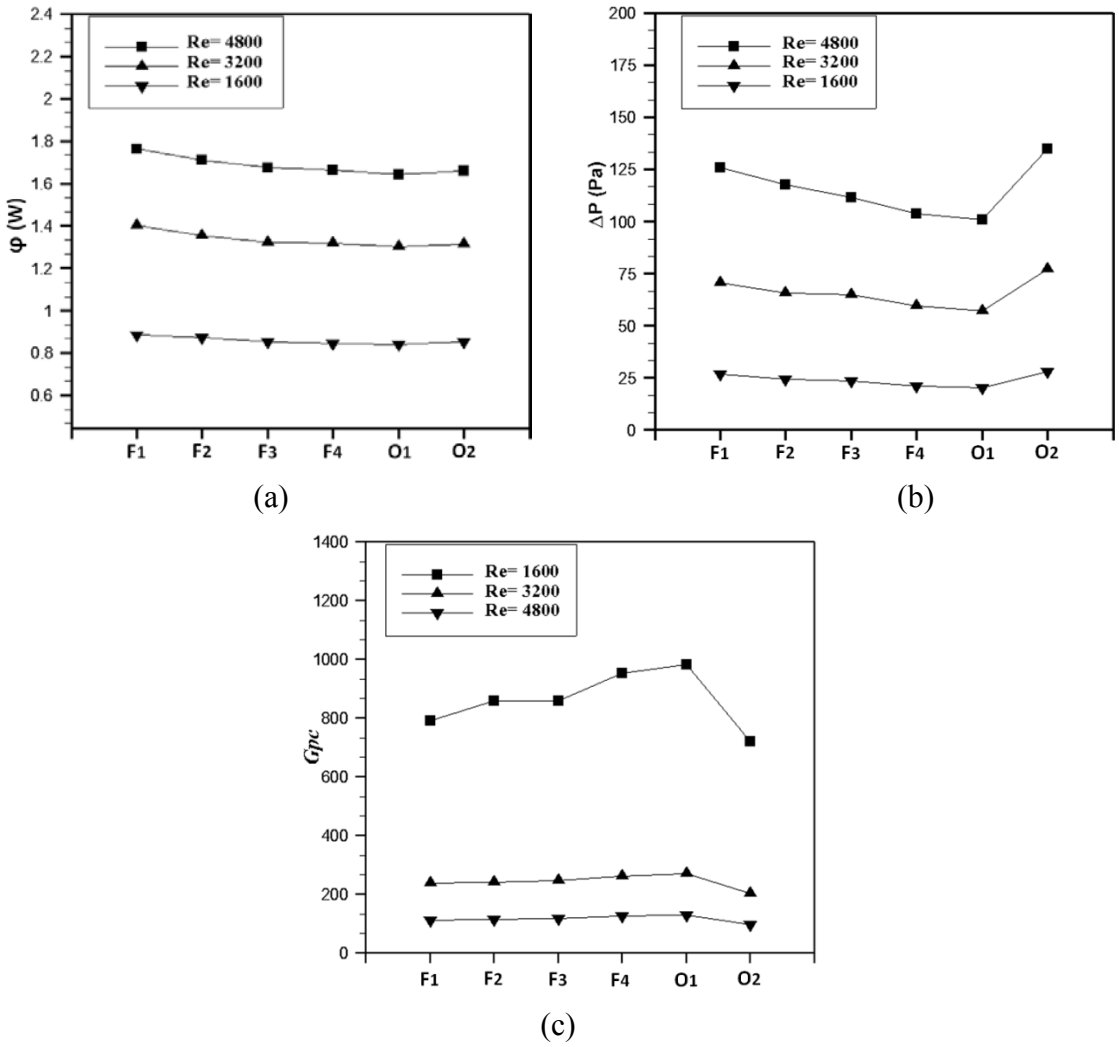

Fig 6.Variation of different performance parameters versus tube shapes and Re (a) heat transfer rate φ ; (b) pressure drop ΔP and (c) global performance criterion G_{PC} .

4. Conclusion

This numerical survey aimed to study the effect of tube geometry and Reynolds number on thermal flow characteristics of sinusoidal wavy FTHEs. For a range of $(1600 \le Re \le 4800)$, the findings were illustrated and compared in terms of heat flux φ, pressure drop ΔP and global performance criterion G_{PC} vs. *Re* number. From the analysis of the numerical results obtained, the main conclusions are listed as follows:

– The tube shape considerably impacts the flow structure between the wavy fins.

– The heat flux φ and the pressure losses ΔP decrease according to the tube flatness, while O1 tube shape reaches, for all Reynolds values, the lowest values of φ and ΔP .

– In terms of the global performance criterion, this parameter increases with the rise of tube flatness and *Re*. For all *Re* values, the G_{pc} values of wavy fins with O1 shaped tubes is the most substantial of all the other tube shapes, being 14.8–24.4% and 31.6–36.3% higher than the fin with F1 and O2 tube geometry, respectively. Therefore, this tube geometry with wavy fins is recommended being used in thermal devices.

5. References

[1] Zeeshan M, Nath S, Bhanja D. Numerical study to predict optimal configuration of fin and tube compact heat exchanger with various tube shapes and spatial arrangements. Energy Conversion and Management 2017; 148:737–16. doi:10.1016/j.enconman.2017.06.011.

[2] Xie G, Wang Q, Sunden B. Parametric study and multiple correlations on air-side heat transfer and friction characteristics of fin-and-tube heat exchangers with large number of large-diameter tube rows. Appl. Thermal Engin 2009;29:1-16. doi:10.1016/ j.applthermaleng. 2008.01.014.

[3] Kumar A, Joshi JB, Nayak AK, Vijayan PK. 3D CFD simulations of air cooled condenser-III: Thermal-hydraulic characteristics and design optimization under forced convection conditions. Heat Mas Transf 2016; 93:1227-21. doi:10.1016/j.ijheatmasstransfer.2015. 10.048.

[4] Kumar A, Joshi JB, Nayak AK. A comparison of thermal-hydraulic performance of various fin patterns using 3D simulations. Int. J. Heat Mass Transf 2017; 109:336–21. doi: 10.1016/j.ijheatmasstransfer.2017.01.102.

[5] Unger S, Beyer M, Gruber S, Willner R, Hampel U. Experimental study on the air-side thermal-flow performance of additively manufactured heat exchangers with novel fin designs. International Journal of Thermal Sciences 2019; 146:106074. doi:10.1016/j.ijthermalsci. 2019.106074.

[6] Zhang L, Tian L, Zhang A, Chen H. Effects of the shape of tube and flow field on fluid flow and heat transfer. Int. Commun. Heat Mass Transf 2020; 117:104782. doi:10.1016/j. icheatmasstransfer.2020.104782.

[7] Brenk A, Kielar J, Malecha Z, Rogala Z. The effect of geometrical modifications to a Shell and tuve heat exchanger on performance and freezing risk during LNG regasification. Int. J. Heat Mass Transf 2020; 161:120247. doi:10.1016/j.ijheatmasstransfer.2020.120247.

[8] Fiebig M, Valencia A, Mitra NK. Local heat transfer and flow losses in fin-and-tube heat exchangers with vortex generators: A comparison of round and flat tubes. Exp. Therm. Fluid Sci 1994; 8:35-11. doi:10.1016/0894-1777(93)90118-3.

[9] Sun L, Zhang CL. Evaluation of elliptical finned-tube heat exchanger performance using CFD and response surface methodology. Int. J. Therm. Sci 2014; 75:45-9. doi: 10.1016/j. ijthermalsci.2013.07.021.

[10] Djeffal F, Bordja L, Rebhi R, Inc M, Ahmad H, Tahrour F, Ameur H, Menni Y, Lorenzini G, Elagan SK, Jawa TM. Numerical investigation of thermal-flow characteristics in heat exchanger with various tube shapes. Appl. Sci. 2021; 11:9477. doi:10.3390/app 11209477.

[11] Unger S, Krepper E, Beyer M, Hampel U. Numerical optimization of a finned tube bundle heat exchanger arrangement for passive spent fuel pool cooling to ambient air. Nucl. Eng. Des. 2020; 361:110549. doi:10.1016/j.nucengdes.2020.110549.

[12] He S, Zhou X, Li F, Wu H, Chen Q, Lan Z. Heat and mass transfer performance of wet air flowing around circular and elliptic tube in plate fin heat exchangers for air cooling. Heat Mass Transf 2019; 55:3661-13. doi:10.1007/s00231-019-02683-1.

[13] Darbari AM, Alavi MA. Application of Taguchi method in the numerical analysis of fluid flow and heat transfer around a flat tube with various axial ratios. Int. Commun. Heat Mass Transf 2021; 126:105472. doi:10.1016/j.icheatmasstransfer.2021.105472.

[14] Alnakeeb MA, Saad MA, Hassab MA. Numerical investigation of thermal and hydraulic performance of fin and flat tube heat exchanger with various aspect ratios. Alex. Eng. J. 2021; 60:4255–11. doi:10.1016/j.aej.2021.03.036.

[15] Phu NM, Pham BT. Thermohydraulic performance of a fin and inclined flat tube heat exchanger: A numerical analysis. CFD Letters 2021; 13(7):1-12. doi:10.37934/cfdl.13.7.112.

[16] Kong Y, Yang L, Du X, Yang Y. Impacts of geometrical structures on thermo-flow performances of plate fin-tube bundles. International Journal of Thermal Sciences 2016; 107:161-18. doi:10.1016/j.ijthermalsci.2016.04.011.

[17] Youn B, Kim NH, An experimental investigation on the airside performance of fin-and-tube heat exchangers having sinusoidal wave fins. Heat Mass Transfer 2007, 43, 1249-1262. doi:10.1007/s00231-006-0210-y.